

**Contribution of Dihydrouridine in Folding of the D-arm in tRNA.**

Journal:	<i>Organic &amp; Biomolecular Chemistry</i>
Manuscript ID:	OB-ART-01-2015-000164.R1
Article Type:	Paper
Date Submitted by the Author:	18-Mar-2015
Complete List of Authors:	Dyubankova, Natalia; Medicinal Chemistry, Rega Institute for Medical Research, KU Leuven, Sochacka, Elzbieta; Lodz University of Technology, Institute of Organic Chemistry Kraszewska, Karina; Centre of Molecular and Macromolecular Studies, Polish Academy of Sciences,, Department of Bioorganic Chemistry Nawrot, Barbara; Centre of Molecular and macromolecular Studies, Polish Academy of Sciences, Department of Bioorganic Chemistry Herdewijn, Piet; Medicinal Chemistry, Rega Institute for Medical Research, KU Leuven, Lescrinier, Eveline; Rega Institute for Medical Research, K.U.Leuven, Laboratory for Medicinal Chemistry,

## ARTICLE

## Contribution of Dihydrouridine in Folding of the D-arm in tRNA.

Cite this: DOI: 10.1039/x0xx00000x

N. Dyubankova,<sup>a</sup> E. Sochacka,<sup>b</sup> K. Kraszewska,<sup>c</sup> B. Nawrot,<sup>c</sup> P. Herdewijn<sup>d</sup> and E. Lescrinier<sup>\*a</sup>Received 00th January 2012,  
Accepted 00th January 2012

DOI: 10.1039/x0xx00000x

www.rsc.org/

Posttranscriptional modifications of transfer RNAs (tRNAs) are proven to be critical for all core aspects of tRNA function. While the majority of tRNA modifications were discovered in the 1970s, their contribution in tRNA folding, stability, and decoding often remains elusive. In this work an NMR study was performed to obtain more insight in the role of the dihydrouridine (D) modification in the D-arm of tRNA<sub>i</sub><sup>Met</sup> from *S. pombe*. While the unmodified oligonucleotide adopted several undefined conformations that interconvert in solution, the presence of a D nucleoside triggered folding into a hairpin with a stable stem and flexible loop region. Apparently the D modification is required in the studied sequence to fold into a stable hairpin. Therefore we conclude that D contributes to the correct folding and stability of D-arm in tRNA. In contrast to what is generally assumed for nucleic acids, the sharp 'imino' signal for the D nucleobase at 10ppm in 90% H<sub>2</sub>O is not indicative for the presence of a stable hydrogen bond. The strong increase in pKa upon loss of the aromatic character in the modified nucleobase slows down the exchange of its 'imino' proton significantly, allowing its observation even in an isolated D nucleoside in 90% H<sub>2</sub>O in acidic to neutral conditions.

### Introduction

Ribosomes in all three kingdoms of life employ aminoacylated tRNA to translate the genetic code in mRNA into a functional peptide. A special methionine tRNA (tRNA<sub>i</sub><sup>Met</sup>) is required for translation initiation. After transcription from DNA but before export to the cytoplasm, tRNA undergoes an extensive folding and modification in the nucleus. It is hypothesized that folding of tRNA into its three-dimensional structure is driven by the formation of tertiary base-pairs rather than by the binding of Mg<sup>2+</sup> and binding pockets for Mg<sup>2+</sup> formed upon the folding process.<sup>1</sup> Theoretical<sup>2</sup> and experimental<sup>3</sup> results indicate the tRNA unfolding is initiated by destruction of contacts between D and T-loops followed by disruption of base pairs in the D-stem.

Folded tRNA, especially in D- and T-loops that form large part of the main body, typically contains Mg<sup>2+</sup> ions and nucleoside modifications.<sup>4</sup> Emerging evidence suggests that a lack of specific body modifications can trigger tRNA degradation in vivo,<sup>5</sup> despite the fact that synthetic unmodified tRNAs are

properly aminoacylated by their cognate synthetases with kinetics similar to those of native tRNA<sup>6</sup> and that unmodified human tRNA<sub>i</sub><sup>Met</sup> is in vitro active in every stage of the initiation processes.<sup>7</sup> More than 90 different tRNA modifications are listed in the RNA Modification Database (<http://mods.rna.albany.edu/>). Modifications in the main body play a role in proper folding of the tRNA into the canonical L-shaped tertiary structure while modifications in or around the anticodon loop contribute to the function of tRNAs in decoding.<sup>8</sup> Those that are found in the core of folded RNA are attributed a role in maintaining the balance between flexibility and stability in tRNA.<sup>9</sup> The presence of modifications in tRNA allows to modulate tRNA across the entire temperature range of natural habitats for microorganisms: in thermophiles specific modifications stabilize folded tRNA to prevent its melting at high temperature while in psychrophilic organisms other modifications maintain a degree of conformational flexibility in tRNA.<sup>10</sup> Among these modified nucleosides, D is highly conserved in the D-loop of tRNAs in the three domains of life.

This nucleoside modification is believed to promote local flexibility in tRNA at low temperature.<sup>11</sup> Its higher abundance in tRNA of low-temperature Archea compared to their thermophilic relatives is in agreement with such a role in maintenance of molecular flexibility of tRNA at low temperatures.<sup>10</sup>

The D modification is formed by a dihydrouridine synthase (Dus) (EC 1.3.1.88) that reduces the carbon-carbon double bond in the uridine base at positions 16 and 17 in tRNA.<sup>12</sup> It is described that the presence of D in the D-loop facilitates mitochondrial tRNA<sup>Leu</sup> folding.<sup>13</sup> Studies have shown that tRNA lacking D (along with other modifications) degrades significantly faster, approaching the degradation rate seen for mRNA<sup>14</sup>, suggesting a role of D in protection of tRNAs from degradation. Studies have indicated that the human Dus2 is responsible for the increased D levels formed in pulmonary carcinogenesis<sup>15</sup> while it was already known for a long time that in cancerous tissues the D levels are increased.<sup>16</sup> Therefore D is thought to play a role in preventing tRNA turnover.

Previously, we already studied the effect of incorporation of N<sup>6</sup>-threonylcarbamoyladenine in the anticodon arm in tRNA<sub>i</sub><sup>met</sup> of *Schizosaccharomyces pombe*.<sup>17</sup> In order to further understand the role of modified nucleosides in this tRNA we now focus on the D modification in its D-arm using NMR spectroscopy and determined the solution structure of a D modified hairpin. Obtained results were compared to spectra of its unmodified counterpart to determine the effects of the nucleoside modification in the studied sequence. Since Mg<sup>2+</sup> has an important role in tRNA folding, changes that are induced by this divalent ion on both modified and unmodified D-arms in solution were monitored.

## Results and Discussion

### The D nucleoside

Dalluge et al. observed in 1996 stabilization of the C2'-endo sugar conformation in a 3'-phosphorylated D. While focusing on the sugar moiety measured in D<sub>2</sub>O, they do not report on the D nucleobase itself. We measured a D nucleoside in 90% H<sub>2</sub>O (+10% D<sub>2</sub>O) since this is a better reference condition for comparison with the D-modified hairpin reported in this work. Surprisingly, the H3 exchangeable proton of the base moiety is nicely visible at 10ppm. The H3 signal was unambiguously assigned in an HMBC spectrum by its three-bond correlation to C5 at 30ppm (Figure 1B).

The drastic reduction in exchange of the 'imino' proton with the solvent can be attributed to an increase of pKa upon reduction of the double bond since deprotonation is the first step in imino proton exchange. A pKa 11.70 for the modified nucleobase was determined by chemical shift changes of C2 and C4 upon increasing pH (Figure 1C). The observed pKa is significantly higher to that of a standard U nucleoside (9.17).<sup>18</sup> Above pH 12.94 the nucleoside quickly decomposes.

Slow exchange of H3 in a D nucleoside makes it observable in 90% H<sub>2</sub>O up to pH 7 (temp 5°C). In contrast to what is

generally assumed on nucleobases, the presence of a sharp 'imino' proton signal of D at 10 ppm at pH 6 is therefore not indicative for its hydrogen bonding. Consequently, the hypothesis of Davis et al.<sup>19</sup> that D has to be involved in specific interactions in tRNA<sub>i</sub><sup>Met</sup>, tRNA<sup>Lys</sup> and tRNA<sup>Phe</sup> based on the observation of its 'imino' proton has to be doubted. In crystal structures of full tRNA molecules containing this nucleoside modification, the D nucleobase is looped out and not involved in hydrogen bonding. Considering the present results on a D nucleoside, an observable 'imino' signal for D does not exclude such a looped out conformation.

Two low energy conformations exist for the 5,6-dihydrouridine ring (depicted in Figure 1D) in the crystal structure of a dihydrouridine nucleoside.<sup>20</sup> Potential energy calculations revealed that for each of these conformations, energy maps for sugar pucker are very similar to those of natural nucleosides.<sup>21</sup> Both conformations would have significantly different splitting of H5 proton signals due to different <sup>3</sup>J couplings with protons in the neighboring CH<sub>2</sub> group. The resolved triplet pattern (<sup>3</sup>J=6.7Hz) for the equivalent H5 protons in the D nucleoside in 90% H<sub>2</sub>O/10% D<sub>2</sub>O indicates that the non-planar nucleobase interconverts fast between both conformations in the studied conditions.<sup>22</sup>

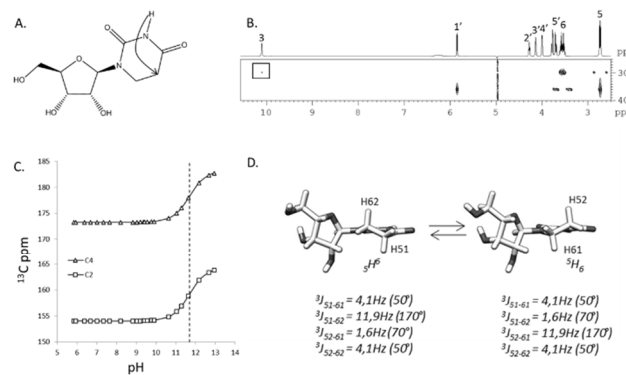


Figure 1: (A) Chemical structure of the studied D nucleoside. The arrow indicates the three bond correlation of H3 to C5 observed in the HMBC spectrum measured at 5°C in 90%H<sub>2</sub>O/10% D<sub>2</sub>O at pH=6 (boxed signal in panel B). Proton assignments are listed along the trace at the top of the 2D section. (C) Chemical shift changes observed for C2 and C4 upon increasing pH. The dashed line corresponds to the determined pKa=11.70. (D) Structures of the two low energy conformations for the 5,6-dihydrouridine ring. Indicative values for <sup>3</sup>J<sub>HH</sub> in the D-ring are calculated<sup>23</sup> from angles between parentheses measured in minimized <sup>5</sup>H<sup>6</sup> and <sup>5</sup>H<sub>6</sub> structures.

### Structure determination of the D-arm including D

A D-arm including a D-modification at position 16 (Figure -2) was investigated by solution NMR methods generally used in RNA structural studies.<sup>24</sup> The non-exchangeable <sup>1</sup>H and <sup>13</sup>C resonances of D-loop were assigned using standard homo- and heteronuclear techniques starting from the anomeric to aromatic proton walk (Figure 3A). The H2 signals in each adenine ring were assigned in an HMBC spectrum in D<sub>2</sub>O by their cross peak to C4 that also correlates to H8<sup>25</sup> which all had expected sequential interactions with H1'(n+1) in a NOESY spectrum with 200ms mixing time (Figure 3A).

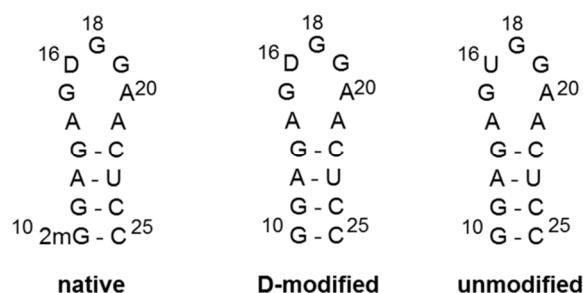


Figure 2: Secondary structure and residue numbering of native, D-modified and unmodified D-arm from tRNA<sub>f</sub><sup>Met</sup> (*S. pombe*).

Typical NMR characteristics of a stable A-form RNA duplex were observed for residues in the stem region, including the sequential walk in the H6/H8-H1' region and in the H6/H8-H2' region of NOESY spectra. The sequential aromatic-to-anomeric NOE interactions are continuous from G10 to A14 and G19 to C25. At 150ms mixing time, the walk is interrupted at A14:H1' to G15:H8, which is significantly broadened compared to other protons in the oligomer.

As initially observed by Nawrot et al.,<sup>26</sup> non-exchangeable protons of the modified nucleobase are observed below 3.8ppm since they do not belong to an aromatic ring. Unfortunately their broadening prevents determination of coupling constants that could be used to determine the conformational state of the 5,6-dihydrouridine ring. This broadening can be attributed to a reduced exchange rate for the inter-conversion between both low energy states of this ring system in the oligo versus the free nucleoside.

The ribose ring of D16 in our loop adopts a *C2'-endo* sugar conformation based on the large  $^3J_{H1'-H2'}$  vicinal coupling (>8Hz) that gives rise to a strong cross peak in the 2D COSY spectrum (Figure 3B). Its 3'-adjacent residues G18 and G19 also have observable cross peaks for H1' to H2' interaction in the 2D-COSY, indicating an increased population of the *C2'-endo* conformation for the ribose rings in these residues. These results are in agreement to what is previously observed in solution on ApDpA and DpUpA trimers,<sup>11, 27</sup> where the preference for a *C2'-endo* conformation in a D nucleoside is propagated to 3'-adjacent residues while preceding residues at the 5'-side retain their common *C3'-endo* conformation. This phenomenon is also observed in residues neighboring D nucleosides in tRNA crystal structures.

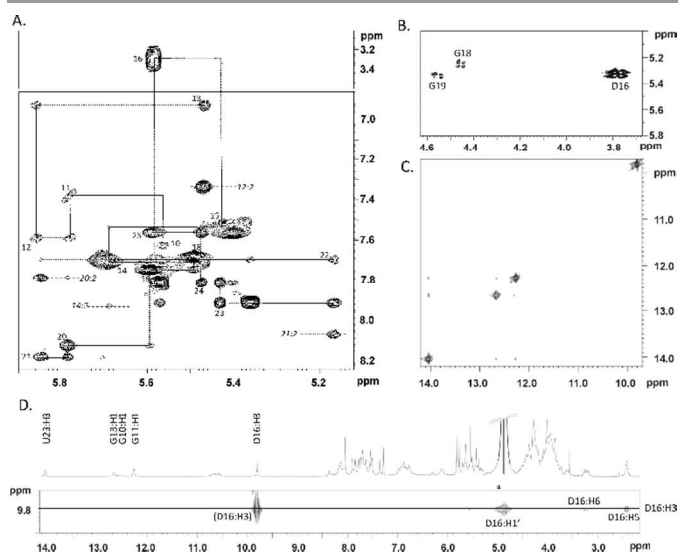


Figure 3: (A) Sections of the NOESY spectrum of the modified D-arm in D<sub>2</sub>O (25°C, 200ms mixing time) covering the anomeric to aromatic proton walk (solid lines); frequencies of adenine:H2 signals are indicated with dashed lines and italic labels. (B) Region of 2D COSY spectrum of D-loop measured in D<sub>2</sub>O at 25°C showing observed H1'-H2' cross peaks. Residue numbering as depicted in Figure 2. (C) Section of a watergateNOESY spectrum in H<sub>2</sub>O/D<sub>2</sub>O 9/1 depicting NOE interactions between iminosignals of the modified D-arm. (D) Strip of a watergateNOESY spectrum in H<sub>2</sub>O/D<sub>2</sub>O 9/1 (mix = 300 ms, 5°C) at the resonance frequency of D16:H3 depicting NOEs of this unusual imino signal. The exchange peak with solvent is indicated with \*. Assigned imino signals are labeled in the trace above the 2D spectrum.

Several exchangeable imino protons are observed between 9 and 14ppm in 90% H<sub>2</sub>O at pH 6 (Figure 3C). Based on their NOE interactions, 4 signals above 11ppm are assigned to Watson-Crick base pairs in the stem while the sharp signal at 9.83 corresponds to the 'imino' proton of D. Since the latter does not have interresidue NOE interactions and its chemical shift is very close that of an isolated D nucleoside, no hydrogen bond restraints were applied for this proton during structure calculation. Two broad signals at ~10.5ppm could not be assigned since they did not have any observable NOE interactions.

The structure of the D-arm was calculated from 294 distance and 54 torsion angle restraints (Figure S1). Starting from an extended strand, a set of 100 structures was generated by torsion angle dynamics. Out of these, 72 structures converged that had no NOE restraint violations >0.5 Å and no torsion angle restraint violations >5°. Ten lowest energy structures of this set were further refined as described in the experimental section (structure statistics reported in table S1).

As can be seen in Figure 4A, the stem region is well defined while the loop covers a relatively large conformational space. This can be due either to the lack of sufficient NMR constraints in this region or an increased flexibility of residues D16, G18 and G19 in solution. The observed COSY cross peaks for H1' to H2' correlations in G18 and G19 (Figure 3B) are indication for puckering of their sugar rings in the applied conditions, supporting the hypothesis on increased flexibility of those

residues. Spin relaxation experiments combined with Heteronuclear Overhauser effect would monitor such an increased flexibility unambiguously, though it was not feasible to perform them on our unlabelled RNA sample. An increased flexibility in the loop region is in agreement with previous observations that D promotes local flexibility in tRNA.<sup>11</sup> The increased abundance of D in tRNA of psychrophilic organisms supports the role of this nucleoside modification in maintenance of molecular flexibility of tRNA at low temperatures.<sup>10</sup>

The stem contains 4 Watson-Crick base pairs and is extended by stacking of A14, G15 and D16 at its 3' side. As was already suspected from the crystal structure of the D nucleoside,<sup>20</sup> the saturated base can participate in stacking interactions similar to those observed in known planar systems. However this stacking is only observed at one side. Apparently, the flexible D nucleobase with its non-planar nature is not apt to be stacked at both sides and therefore induces a turn in the hairpin loop. At its 5' side stacking of Watson-Crick base-paired residues in the stem is extended to of A21, A20 and G19 in all calculated structures while even G18 tends to stack on G19 in some of the calculated structures (2 out of 10).

No hydrogen bonds were applied in loop residues, however the pairs G15 – A20 and A14 - A21 tend to adopt a coplanar conformation. In the lowest energy structure, hydrogen bonding occurs for sheared G15-A20 base pair, while A14:N6 and A21:N1 are also within hydrogen bonding distance (Figure 4C and D). Observed NOE interactions of nucleobase protons support these configurations. The *syn* orientation of A20 is in agreement with its strong intrasidic NOE from H8 to H1' and weak NOE of H8 to H2' and H3'. The strong NOE interaction that occurs between H2 protons in residues 21 and 14 supports position of their nucleobases as depicted in Figure 4D.

In the high resolution tRNA crystal structure of yeast phenylalanine tRNA,<sup>28</sup> D adopts a <sup>5</sup>H<sub>6</sub> conformation while in our final NMR structures this non-planar ring adopts a <sup>3</sup>H<sub>6</sub> conformation. According to the appearance of the signal from H5 protons in D, an equilibrium between both low energy states is expected, though this is not reflected in the final structures. Observed NOE interactions most likely favour one of the conformations during torsion angle dynamics. A comparable preference for a C3'-endo sugar conformation in riboses of G18 and G19 is observed in the calculated structures ( $\delta$  torsion angles reported in Table S2) despite of their observed average values for <sup>3</sup>J<sub>H1'-H2'</sub> and the absence of dihedral restraints on those residues during structure calculation.

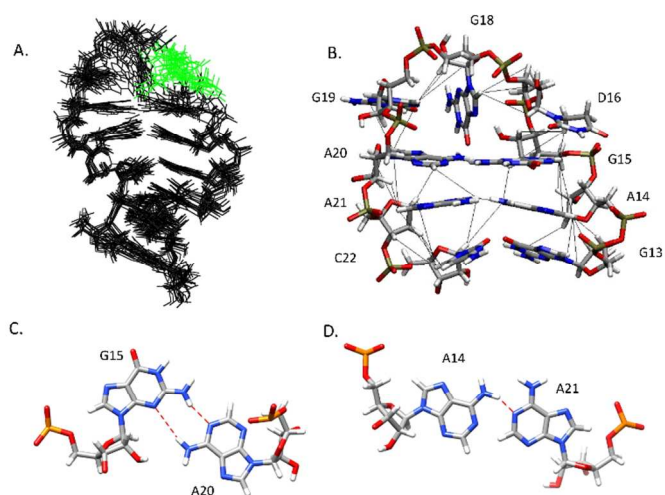


Figure 4: (A) Overlay of the 10 lowest energy structures fitted to all residues. (B) Focus on the loop region of the lowest energy structure calculated for the modified D-arm. Important interresidue NOE interactions are indicated by black lines. (C) Sheared G15-A20 base pair in the lowest energy structure. (D) 'N1-amino' hydrogen bond in the A14-A21 base pair in the lowest energy structure.

#### Comparison of modified and unmodified D-arm

While the modified D-arm folded into a stable hairpin, its uridine-containing homologue adopted interconverting conformations in solution, causing exchange crosspeaks in 2D ROESY, line broadening in 1D spectra (Figure 5) and extra imino signals. A DOSY experiment was performed to determine the diffusion coefficient for both oligonucleotides in solution. The measured diffusion constant of the D-modified arm ( $1.9(0.2) \times 10^{-6} \text{ cm}^2/\text{s}$ ) is in agreement with a hairpin while the observed value of the unmodified sequence ( $1.5(0.1) \times 10^{-6} \text{ cm}^2/\text{s}$ ) indicates that at least a portion of the unmodified oligo is in a duplex state.<sup>29</sup> After determining the crystal structure of a D nucleoside, it was already suggested that a D nucleoside would promote a 'loop' formation in the sugar-phosphate chain since they observed an unusual conformational preference for the torsion angle about the C4'-C5' bond.<sup>30</sup> More recently it was demonstrated that the T<sub>m</sub> of RNA duplexes is decreased with a D unit in its central part.<sup>31</sup> This effect was attributed to destabilizing effect of a D nucleobase on the C3'-endo sugar conformation typical for double stranded A-type RNA<sup>11</sup> and its non-planar nature disturbing stacking interactions with neighboring nucleobases. Those disfavouring effects of D on duplex formation are probably the driving force for the modified D-arm to adopt exclusively the hairpin conformation in solution.

Regarding the role of divalent ions during tRNA folding, we monitored the effect of Mg<sup>2+</sup> on spectra of both modified and unmodified D-arm. Upon adding Mg<sup>2+</sup>, line broadening of signals from the unmodified oligo decreased allowing to distinguish two different sets of signals. The monomer/dimer ratio of this oligomer was not influenced by the presence of Mg<sup>2+</sup> since increasing concentrations of Mg<sup>2+</sup> did not alter the measured diffusion rate of the unmodified oligo.

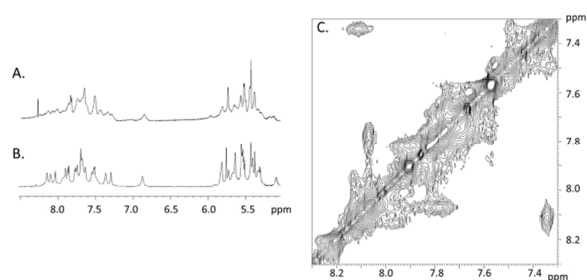


Figure 5: Region of 1D proton spectra in  $D_2O$  of unmodified (A) and D-modified (B) D-arm measured in  $D_2O$  at  $20^\circ C$ . (C) Section of the ROESY spectrum measured on the unmodified D-arm showing strong exchange cross peaks for aromatic signals.

Adding  $Mg^{2+}$  to the D-modified D-arm induced consistent chemical shift changes in G18, A19, A20, C22 and A21 (sorted from weak to strong effect, Figure S2). Unfortunately we could not increase  $Mg^{2+}$  above 2.5 mM due to precipitation. The gradual shift of specific signals suggests that a fast exchange regime is established between  $Mg^{2+}$  bound and unbound form of the D-modified oligomer upon adding the divalent ion. Precipitation at  $[Mg^{2+}] = 2.5 \text{ mM}$  combined with the relatively strong changes that are observed (especially in C22 and A21) within the  $[Mg^{2+}]$  range that could be covered, suggest that upon binding  $Mg^{2+}$  a conformational change takes place that induces aggregation. No changes were observed for NOE interactions within the oligo for  $[Mg^{2+}]$  up to 2.5 mM, indicating that the unbound form is still the most abundant in solution at these conditions.

## Materials and Methods

### Sample preparation

An unlabeled RNA oligomer 5'-GGAGAGUGGAACUCC-3' (the non-modified D-arm) was obtained from Eurogentec S.A. (Belgium). A modified RNA oligonucleotide 5'-GGAGAGDGGAAACUCC-3' (15-mer) containing 5,6-dihydrouridine unit (D) was synthesized on an ÅKTA<sup>TM</sup> oligopilot synthesizer (GE Healthcare, Uppsala, Sweden) at 16.5  $\mu\text{mol}$  scale by the standard phosphoramidite approach. Primer Support 200<sup>TM</sup> loaded with a 5'-DMT- $C^{Ac}$  monomer and TheraPure<sup>TM</sup> UltraMild phosphoramidite monomers of adenosine (2'-TBDMSi- $A^{PAC}$ ), cytidine (2'-TBDMSi- $C^{Ac}$ ), guanosine (2'-TBDMSi- $G^{iPrPAC}$ ), and uridine (2'-TBDMSi-U) (ThermoFisher), as well as 5'-*O*-dimethoxytrityl-5,6-dihydrouridine, 2'-*O*-TBDMSi-3'-[(2-cyanoethyl)-(N,N-diisopropyl)]-phosphoramidite, prepared as described previously<sup>31, 32</sup> were used as the components in the synthesis. For all monomers a 15 min coupling time was applied, and the capping step was done with *N*-methylimidazole/phenoxycetic anhydride in sym-collidine/acetonitrile solvent system. The 5'-terminal DMT-OFF oligonucleotide was released from the support by basic deprotection (treatment with anhydrous 2M ammonia in methanol, 16 hours at  $30^\circ C$ ) and the solid support

was washed extensively with methanol. After evaporation the sample was resuspended in anhydrous TEA  $\times$  3HF / DMF (10:3, v/v) mixture and kept for 24 hours at room temperature. The reaction was quenched with DEPC-treated water and the RNA was precipitated with isopropyl trimethylsilyl ether at room temperature and, after addition of diethyl ether, separated by centrifugation at  $4^\circ C$ . The crude RNA pellet was purified by ion-exchange HPLC (semipreparative Q column), in perchlorate buffer system<sup>33</sup> and desalted on C-18 SepPak<sup>TM</sup> cartridges to yield 234 OD of the product. The calculated molecular weight of the RNA oligonucleotide (4856.03 g/mol) was confirmed by MALDI-TOF MS ( $m/z$  4857.1).

Samples were lyophilized and dissolved in 0.75 ml in a 90%/10% mixture  $H_2O/D_2O$  and pH was adjusted to 6.8 by adding small amounts of 0.01N HCl in  $H_2O$ , yielding a 2 mM oligonucleotide concentrations for each of oligo's. For recording spectra in  $D_2O$ , the samples were lyophilized and dissolved in a 0.75 ml 100%  $D_2O$  mixture. Oligonucleotide solutions were annealed prior to NMR experiments by short heating at  $80^\circ C$  and fast cooling on ice to promote hairpin formation. Initially, no additional salts or buffer were added to avoid conditions that would favour duplex formation.

### NMR experiments

A Bruker Avance 500 spectrometer equipped with a TXI Z gradient probe was used to obtain spectra involving phosphorus nuclei. Other spectra were recorded on a Bruker Avance II 600MHz spectrometer using a 5 mm TXI HCN Z gradient cryoprobe.

The water signal in samples with 90%  $H_2O$  was suppressed using excitation sculpting<sup>34</sup>. The 2D NOESY in 90%  $H_2O$  (mixing times = 200 ms; at  $5^\circ C$ ) was recorded with a sweep width of 14400 Hz in both dimensions, 2048 data points in  $t_2$  and 256 FIDs in  $t_1$ . The data were apodized with a shifted sine-bell square function in both dimensions.

The 2D DQF-COSY<sup>35</sup>, TOCSY<sup>36</sup> and NOESY<sup>37</sup> spectra in  $D_2O$  were recorded with a sweep width of 5400 Hz in both dimensions. The total TOCSY mixing time was set to 64 ms. All spectra were acquired with 2048 data points in ( $t_2$ ) and 512 FIDs in ( $t_1$ ). The data were apodized with a shifted sine-bell square function in both dimensions and processed to a 4K x 1K matrix. The NOESY experiments were acquired with mixing times of 100, 150 and 300ms.

All [ $^1H$ - $^{31}P$ ]-HETCOR<sup>38</sup> spectra were acquired with 2048 data points in the proton dimension,  $t_2$  and 512 increments in the phosphorus dimension,  $t_1$ , over sweep widths of 5400 and 2430 Hz, respectively. The data were apodized with a shifted sine-bell square function in both dimensions and processed to a 2K x 1K matrix.

Natural abundance [ $^1H$ ,  $^{13}C$ ]-HSQC<sup>39</sup> were recorded with sensitivity enhancement and gradient coherence selection optimized for selection of CH groups ( $^1J_{CH} = 150\text{Hz}$ ) using 256/1024 complex data points and 60/9 ppm spectral widths in  $t_1$  and  $t_2$ , respectively to measure  $^1H$ - $^{13}C$  correlations in the sugar part of the nucleosides and H5-C5 correlations in pyrimidine nucleobases. A separate natural abundance [ $^1H$ ,  $^{13}C$ ]-

HSQC was measured to determine the remaining  $^1\text{H}$ - $^{13}\text{C}$  correlations in nucleobases. It was optimized for selection of aromatic CH groups ( $^1J_{\text{CH}} = 180\text{Hz}$ ) using 128/1024 complex data points and 40/9 ppm spectral widths in  $t_1$  and  $t_2$ , respectively.

Natural abundance [ $^1\text{H}$ ,  $^{13}\text{C}$ ]-HMBC were measured in  $\text{D}_2\text{O}$  to correlate H2 and H8 protons to in adenine<sup>25</sup> using 4096/128 complex data points and 10/60 ppm spectral widths in  $t_2$  and  $t_1$ , respectively ( $^1J_{\text{CH}} = 200\text{Hz}$  and  $^3J_{\text{CH}} = 8\text{Hz}$ ).

The Bruker pulse sequence ledbpgp2spr (2D 1H DOSY double stimulated-echo including solvent presaturation) was used to measure diffusion coefficients through DOSY NMR experiments. The longitudinal eddy current delay and the gradient recovery delay were kept at fixed values of 5 and 0.1 ms, respectively. The diffusion-sensitive period ( $\Delta$ ) and the gradient duration ( $\delta$ ) were optimized to 300ms and 3ms respectively, allowing the signals of interest to decrease by a factor of 10–20, in order to better characterize the signal exponential decay predicted by the Stejskal–Tanner expression.<sup>40</sup>

### NMR resonance assignment

Standard methods were applied to assign non-exchangeable protons starting from a classic anomeric-to-aromatic proton walk<sup>41</sup> From TOCSY, DQF-COSY and NOESY spectra, assignment of remaining proton signals in sugar rings could be established. Heteronuclear experiments on natural abundance samples were performed for assignment of  $^{13}\text{C}$  and  $^{31}\text{P}$  signals. Signals of exchangeable imino protons were assigned using sequential imino–imino interactions and imino–aromatic contacts observed in a NOESY spectrum collected in 90%  $\text{H}_2\text{O}/10\%$   $\text{D}_2\text{O}$ .

### NMR restraints

Distance restraints between non-exchangeable protons were derived from NOESY spectrum 100 ms mixing times. Based on ISPA, inter-proton distances were calculated. An experimental error ( $\pm 20\%$ ) was used on the calculated inter-proton distances. The calibration of NOE cross peak intensities was done against the H5–H6 cross peaks as an internal standard. The distances involving exchangeable protons were collected from NOESY spectrum in 90%  $\text{H}_2\text{O}$  and manually set to 1.0–2.0 Å, 1.0–3.6 Å and 1.0–5.0 Å for strong medium and weak cross-peaks intensities respectively.

Sugar puckers of the riboses were inferred from the weak H1' to H2' scalar couplings. Residues that have H1' to H2' scalar couplings varying from 0 and 2 Hz were restrained to the N pucker conformation [dihedral restraints applied: H1'-C1'-C2'-H2' ( $99.2 \pm 20^\circ$ ), H2'-C2'-C3'-H3' ( $39.4 \pm 20^\circ$ ), H3'-C3'-C4'-H4' ( $-162.0 \pm 20^\circ$ )]. In residues that have larger H1' to H2' couplings (between 3 and 7 Hz), no restraints were applied on the sugar rings of these residues during the structure calculation.

The normal  $^{31}\text{P}$  chemical shifts of base paired residues in the stem were used to restrain  $\alpha$  and  $\zeta$  torsion angles ( $0 \pm 120^\circ$ ).

The  $\epsilon$  torsion angles were restrained (to  $230^\circ \pm 70^\circ$ ) based on steric arguments.<sup>42</sup>

Hydrogen bond restraints in Watson-Crick base pairs of the stem with unambiguously assigned imino signals, were applied as NOE-distance restraints.

### NMR Structure calculations

Structure calculations were performed with X-PLOR-NIH V3.851.<sup>43</sup> A set of 100 structures was generated by torsion angle molecular dynamics, starting from an extended strand and using NMR derived restraints. Ten lowest energy structures were used for further refinement during the 'gentle molecular dynamics' round in water.<sup>44</sup> The obtained structures were analyzed with the Curves+ program (version 1.31).<sup>45</sup>

### Conclusions

The D-arm forms a major part in the core of tRNA where it is involved in tertiary interactions and  $\text{Mg}^{2+}$  binding that are important in tRNA folding. Within all kingdoms of life the D modification in the loop region of this arm is highly conserved and hence its name. Our results demonstrate that in the studied sequence the presence of D is required to fold into a stable hairpin with a flexible loop that is able to bind  $\text{Mg}^{2+}$ . When evaluating the structure of the modified hairpin, we conclude that the flexible nature of D with its non-planar base favours formation of a hairpin over a duplex. The modified D-loop itself is a point of local structural dynamics which is in agreement with the observation that D enhances local tRNA flexibility (9). Whether the binding of  $\text{Mg}^{2+}$  by the D-modified stem-loop has a functional role in tRNA folding remains a subject for further studies.

### Acknowledgements

The authors thank Dr Peter Guterstam, GE Healthcare, Uppsala, Sweden for the large scale synthesis of dihydrouridine-containing RNA oligonucleotide. The refined coordinates of the ten lowest energy structures are deposited in the PDB database (accession number: 2mn0) together with measured chemical shifts and experimental restraints. This work was partly funded by FWO (Flemish fund for scientific research) [G.0664.12] and GOA (KUL Research fund) [GOA/10/13] grants and by Statutory Funds of CMMS PAS and TUL in Poland.

### Notes and references

<sup>a</sup> Medicinal Chemistry, Department of Pharmaceutical Sciences, Rega Institute for Medical Research, KU Leuven, Minderbroedersstraat 10, 3000 Leuven, Belgium.

<sup>b</sup> Institute of Organic Chemistry, Faculty of Chemistry, Technical University of Lodz, Zeromskiego 116, 90-924 Lodz, Poland.

<sup>c</sup> Department of Bioorganic Chemistry, Centre of Molecular and Macromolecular Studies, Polish Academy of Sciences, Sienkiewicza 112, 90-363 Lodz, Poland.

Electronic Supplementary Information (ESI) available: complementary NMR and structural data. See DOI: 10.1039/b000000x/

1. L. Jovine, S. Djordjevic and D. Rhodes, *J. Mol. Biol.*, 2000, 301, 401-414.
2. L. B. Pereyaslavets, M. V. Baranov, E. I. Leonova and O. V. Galzitskaya, *Biochemistry (Mosc)*, 2011, 76, 236-244.
3. E. J. Maglott, J. T. Goodwin and G. D. Glick, *J. Am. Chem. Soc.*, 1999, 121, 7461-7462.
4. W. B. Derrick and J. Horowitz, *Nucleic Acids Res.*, 1993, 21, 4948-4953.
5. E. M. Phizicky and A. K. Hopper, *Genes Dev.*, 2010, 24, 1832-1860.
6. L. H. Schulman, *Prog. Nucleic Acid Res. Mol. Biol.*, 1991, 41, 23-87.
7. T. V. Pestova and C. U. Hellen, *RNA*, 2001, 7, 1496-1505.
8. J. E. Jackman and J. D. Alfonzo, *Wiley Interdiscip. Rev. RNA*, 2013, 4, 35-48.
9. K. Ishida, T. Kunibayashi, C. Tomikawa, A. Ochi, T. Kanai, A. Hirata, C. Iwashita and H. Hori, *Nucleic Acids Res.*, 2011, 39, 2304-2318.
10. K. R. Noon, R. Guymon, P. F. Crain, J. A. McCloskey, M. Thomm, J. Lim and R. Cavicchioli, *J. Bacteriol.*, 2003, 185, 5483-5490.
11. J. J. Dalluge, T. Hashizume, A. E. Sopchik, J. A. McCloskey and D. R. Davis, *Nucleic Acids Res.*, 1996, 24, 1073-1079.
12. F. Yu, Y. Tanaka, K. Yamashita, T. Suzuki, A. Nakamura, N. Hirano, T. Suzuki, M. Yao and I. Tanaka, *Proc. Natl. Acad. Sci. USA*, 2011, 108, 19593-19598.
13. C. I. Jones, A. C. Spencer, J. L. Hsu, L. L. Spemulli, S. A. Martinis, M. DeRider and P. F. Agris, *J. Mol. Biol.*, 2006, 362, 771-786.
14. A. Alexandrov, I. Chernyakov, W. Gu, S. L. Hiley, T. R. Hughes, E. J. Grayhack and E. M. Phizicky, *Mol. Cell*, 21, 87-96.
15. T. Kato, Y. Daigo, S. Hayama, N. Ishikawa, T. Yamabuki, T. Ito, M. Miyamoto, S. Kondo and Y. Nakamura, *Cancer Res.*, 2005, 65, 5638-5646.
16. Y. Kuchino and E. Borek, *Nature*, 1978, 271, 126-129.
17. E. Lescrinier, K. Nauwelaerts, K. Zanier, K. Poesen, M. Sattler and P. Herdewijn, *Nucleic Acids Res.*, 2006, 34, 2878-2886.
18. J. Baddiley, in *The nucleic acids: chemistry and biology. Edited by Erwin Chargaff [and] J.D. Davidson*, eds. E. Chargaff and J. N. Davidson, Academic Press, New York, 1955, vol. 1, pp. 137-190.
19. D. R. Davis and C. D. Poulter, *Biochemistry*, 1991, 30, 4223-4231.
20. M. Sundaralingam, S. T. Rao and J. Abola, *J. Am. Chem. Soc.*, 1971, 93, 7055-7062.
21. P. K. Ponnuswamy and A. Anukanth, *J. Theor. Biol.*, 1982, 96, 233-251.
22. H. Friebolin, in *Basic One and Two Dimensional NMR Spectroscopy*, ed. H. Friebolin, VCH, Weinheim, Germany, 1991, ch. 9.4.2, pp. 263-266.
23. C. A. G. Haasnoot, F. A. A. M. Deleeuw and C. Altona, *Tetrahedron*, 1980, 36, 2783-2792.
24. M. P. Latham, D. J. Brown, S. A. McCallum and A. Pardi, *ChemBioChem*, 2005, 6, 1492-1505.
25. M. J. van Dongen, S. S. Wijmenga, R. Eritja, F. Azorin and C. W. Hilbers, *J. Biomol. NMR*, 1996, 8, 207-212.
26. B. Nawrot, A. Malkiewicz, W. S. Smith, H. Sierzputowska-Gracz and P. F. Agris, *Nucleos. Nucleot.*, 1995, 14, 143-165.
27. J. W. Stuart, M. M. Basti, W. S. Smith, B. Forrest, R. Guenther, H. SierzputowskaGracz, B. Nawrot, A. Malkiewicz and P. F. Agris, *Nucleos. Nucleot.*, 1996, 15, 1009-1028.
28. H. Shi and P. B. Moore, *RNA*, 2000, 6, 1091-1105.
29. J. Lapham, J. P. Rife, P. B. Moore and D. M. Crothers, *J. Biomol. NMR*, 1997, 10, 255-262.
30. M. Sundaralingam, S. T. Rao and J. Abola, *Science*, 1971, 172, 725-727.
31. K. Sipa, E. Sochacka, J. Kazmierczak-Baranska, M. Maszewska, M. Janicka, G. Nowak and B. Nawrot, *RNA*, 2007, 13, 1301-1316.
32. B. Nawrot and E. Sochacka, *Curr. Protoc. Nucleic Acid Chem.*, 2009, Chapter 16, Unit 16 12.
33. B. Sproat, in *Methods in Molecular Biology*, ed. P. Herdewijn, Humana Press Inc., Totowa, NJ., 2004, vol. 288, pp. 17-31.
34. P. Plateau and M. Gueron, *J. Am. Chem. Soc.*, 1982, 104, 7310-7311.
35. M. Rance, O. W. Sørensen, G. Bodenhausen, G. Wagner, R. R. Ernst and K. Wüthrich, *Biochem. Biophys. Res. Commun.*, 1983, 117, 479-485.
36. A. Bax and D. G. Davis, *J. Magn. Reson.*, 1985, 65, 355-360.
37. J. Jeener, B. H. Meier, P. Bachmann and R. R. Ernst, *J. Chem. Phys.*, 1979, 71, 4546-4553.
38. V. Sklenar, H. Miyashiro, G. Zon, H. T. Miles and A. Bax, *FEBS Lett.*, 1986, 208, 94-98.
39. J. Schleichner, M. Schwendinger, M. Sattler, P. Schmidt, O. Schedletsky, S. J. Glaser, O. W. Sorensen and C. Griesinger, *J. Biomol. NMR*, 1994, 4, 301-306.
40. D. Sinnaeve, *Concept. Magn. Reson A*, 2012, 40A, 39-65.
41. S. S. M. Wijmenga, M.W.; Hilbers, C.W., in *NMR of Macromolecules, a Practical Approach*, ed. G. C. K. Roberts, Oxford University Press, Oxford, UK, 1993, pp. 217-288.
42. S. S. Wijmenga and B. N. M. van Buuren, *Prog. Nuc.l Mag. Res. Sp.*, 1998, 32, 287-387.
43. C. D. Schwieters, J. J. Kuszewski, N. Tjandra and G. M. Clore, *J. Magn. Reson.*, 2003, 160, 65-73.
44. J. P. Linge, M. A. Williams, C. A. E. M. Spronk, A. M. J. J. Bonvin and M. Nilges, *Proteins*, 2003, 50, 496-506.
45. R. Lavery, M. Moakher, J. H. Maddocks, D. Petkeviciute and K. Zakrzewska, *Nucleic Acids Res.*, 2009, 37, 5917-5929.